Eng. & Technology, Vol.24, No.2, 2005

Estimating Image Blur Using Discrete Multiwavelet Transform

Dr. Matheel Emad AL-Deen Abdulmunim

Received on: 1/8/2004
Accepted on: 28/11/2004

Abstract:

In this paper, a multiwavelet based method is proposed to estimate the blur in an image using information contained in the image itself. We look at the sharpness of the sharpest edges in the blurred image, which contain information about the blurring. Specifically, a smoothness measure, the Lipschitz exponent, is computed for these sharpest edges. A relation between the variance of a gaussian point spread function and the magnitude of the Lipschitz exponent is shown, which is only dependent on the blur in the image and not on the image contents. This allows us to estimate the variance of the blur directly from the image itself.

تخمين تضبب الصورة باستخدام النقل المتقطع متعدد المويجات

الخلاصة:

في هذا البحث اقترحت طريقة معتمدة على متعدد المويجات لتخمين التضبب في الصورة باستخدام المعلومات المتضمنة في الصورة نفسها. وقد تم النظر الى الحدية لأكثر الحواف حدة بالصورة المضببة والتي تضم معلومات حول التضبيب. وبشكل خاص فقد تم حساب مقياس التنعيم (اس ليجتس) لتلك الحواف الأكثر حدية. ووضحت العلاقة بين الأختلاف لدالة انتشار النقاط لكاوس و بين مرتبة اس ليجتس والمعتمدة فقط على التضبب في الصورة وليس على محتويات الصورة. وهذا يمكننا من تخمين الأختلاف للتضبب بشكل مباشر من الصورة نفسها.

Keywords: Multiwavelet transform, blurring, image processing.

1 Introduction:

Blurring of edges in an image occurs in many different fields. Image blur is modelled as [1]:

$$g(x,y) = (h * f)(x,y) \quad \ldots(1)$$

with $g(x,y)$ the blurred image, $f(x,y)$ the unknown sharp image and $h(x,y)$ the point spread function (PSF). The symbol (*) represents the convolution operator, and models the image blur. It is in fact the response of the imaging system to an ideal point source.

This blur is often unwanted and has to be compensated for (this is image restoration, and is applied in astronomy, medical imaging, microscopy, ...). In that case, the estimation of the blur is needed to restore the ideal image $f(x,y)$ from degraded data $g(x,y)$. Sometimes however, this blur contains extra information. For example, it can provide information about the settings of the camera.

When dealing with autofocus cameras, one expects to find a sharp image, because all natural images contain sharp edges since an object in front of a background produce sharp edges. When an image is out of focus, the sharpness of the sharpest edges that are still present in the image gives us information about how much an out-of-focus camera needs to be adjusted.

Blurred edges can also provide information about the 3D nature of the scene itself. In those applications, depth is estimated from focus/defocus [1,2].

* Applied Science Dept., University of Technology
Matheel74@netzero.com

https://doi.org/10.30684/etj.24.2A.6
2412-0758/University of Technology-Iraq, Baghdad, Iraq

Again, we assume that all objects in front of a background have sharp edges. But only objects in the focal plane are imaged with sharp edges. For objects not in the focal plane these sharp edges will be blurred proportionally to their distance from the focal plane, thus providing some depth information about the image.

In this paper, a method is proposed to estimate the PSF in an image by looking how sharp the sharpest edges in a blurred image still are, in order to find information about the PSF. It estimates in particular the variance σ_{bl} of a Gaussian PSF from information contained in the image itself [3]:

$$\mathrm{PSF}(x,y) = \frac{1}{\sqrt{2\pi}\sigma_{bl}} e^{-(x^2+y^2)/(2\sigma_{bl}^2)} \qquad \ldots(2)$$

Our method can estimate the image blur with an accuracy of about 10%. Other techniques for blur estimation using Gaussian PSF's [3,4] use derivatives of the Gaussian PSF to determine the variance of the Gaussian blur. We present an alternative method, which doesn't use derivatives, but a measure of the smoothness of the image at a certain position.

This method can also be extended to Gaussian PSF's that are not axially symmetrical and even to PSF's that aren't even gaussian. For out-of-focus blur, a uniform circular PSF is used [5,6]. Our method requires only minor modifications to adapt to this kind of PSF, as will be shown in the paper.

2 Multiwavelets:

As in the scalar wavelet case, the theory of multiwavelets is based on the idea of multiresolution analysis (MRA).

The difference is that multiwavelets have several scaling functions. The standard multiresolution has one scaling function Ø(t) [7].

i. The translates Ø(t – k) are linearly independent and produce a basis of the subspace V_0.

ii. The dilates Ø(2^j t–k) generate subspaces V_j, j ∈Z, such that:

$$\ldots \subset V_{-1} \subset V_0 \subset V_1 \subset V_j \subset \ldots \qquad \ldots(3)$$

$$\overline{\bigcup_{j=-\infty}^{\infty} V_j} = L^2(R), \quad \bigcap_{j=-\infty}^{\infty} V_j = \{0\}$$

iii. There is one wavelet w(t). Its translates w(t – k) produce a basis of the "detail" subspace W_0 to give V_1:

$$V_1 = V_0 \oplus W_0 \qquad \ldots(4)$$

For multiwavelets, the notion of MRA is the same except that now a basis for V_0 is generated by translates of N scaling functions Ø$_1$(t – k), Ø$_2$(t – k), …, Ø$_N$(t – k). The vector Ø(t) = [Ø$_1$(t), …, Ø$_N$(t),]^T, will satisfy a matrix dilation equation (analogous to the scalar case)

$$\Phi(t) = \sum_k C[k]\Phi(2t-k) \qquad \ldots(5)$$

The coefficients C[k] are N by N matrices instead of scalars. Associated with these scaling functions are N wavelets w_1(t), …, w_N(t), satisfying the matrix wavelet equation:

$$W(t) = \sum_k D[k]\Phi(2t-k) \qquad \ldots(6)$$

Again, W(t)= [w_1(t), …, w_N(t)] ^{T} is a vector and the D[k] are N by N matrices [7].

3 The Proposed Method Principle:

The proposed method for blur estimation is based on estimating the sharpness of the sharpest edges in the image. To analyze edges in the image, we calculate the Lipschitz exponent in all

points where a change in intensity is found either in the horizontal or vertical direction.

The Lipschitz exponent (sometimes referred to as Holder exponent) is a measure of how smooth the image is in a certain point. In fact, it is an extension of how many times the image is differentiable in a certain point. For example, a signal that is differentiable once, has Lipschitz exponent 1, a step function has Lipschitz 0 and a dirac impulse Lipschitz -1. In the multiwavelet domain, it is possible to calculate the Lipschitz exponent in a certain point in the image from the evolution of the modulus maxima of the multiwavelet coefficients corresponding to that point through successive scales. Mallat has shown in [8–10] how Lipschitz regularity van be calculated for a one-dimensional signal.

Consider the cone of influence for a point v. The cone of influence in v (fig. 1) are the points (u,s) in scale-place space that are within the support of the multiwavelet $\psi_{v,s}$ at position v and scale s.

Now, if the signal is uniformly Lipschitz α in the neighbourhood of a certain point v, then a constant A exists such that all multiwavelet coefficients within the cone of influence around v in the scale-place space satisfy the condition

$$\max(|Wf(u,s)|) = A\, s^{\alpha+1/2}, \quad \ldots(7)$$

$$\therefore \log_2 Max(|wf(u,s)|) = \log_2 A + (\alpha + 1/2)\log_2 s \quad \ldots(8)$$

Here, $W|f(u,s|$ represents the modulus of the multiwavelet transforms of $f(x)$ at resolution scale s. The Lipschitz regularity in at v is given by the maximum slope of $\log_2|W f(v,s,x)|$ as a function of $\log_2 s$ along the lines of modulus maxima that converge towards v within the cone of influence.

4 Practical considerations:

The multiwavelet decomposition of the image is calculated, and by following the modulus maxima of the multiwavelet coefficients corresponding to a certain point in the image through different resolution scales, the Lipschitz exponent in that point is calculated by fitting an exponential curve to the modulus maxima versus the scale, as described earlier [8–10]. A problem in this approach is that even minor intensity variations in smooth regions result in Lipschitz exponents that correspond with sharp edges. An example is shown in fig. (2). In the mirror region at the right of the famous 'Lena' image, we can see what causes this effect. When magnified and with enhanced contrast, we see the intensity variations, even in apparently smooth regions.

The problem is to distinguish sharp transitions which a small amplitude from smooth transitions. This disturbs our estimation of the blurring of the image. However, transitions with small amplitude are not likely to belong to dominant image features.

Because we work in the multiwavelet domain, we restrict our analysis to features that produce a gradient above a certain threshold. This gradient is extracted from the multiwavelet detail coefficients in the highest resolution scale. The threshold was determined empirically so that major image features were visible. Empirically, this thresholds corresponds with $30/\sigma_{bl}$.

From the Lipschitz exponents thus found along the significant edges in the image, a histogram is made. For this histogram, we divided the range of

Lipschitz exponents in intervals with a width of 0.1. Because we restricted the lipschitz exponents to those corresponding with transitions with large amplitude, we already filtered out the sharpest transitions with large amplitude in the image.

When we make a histogram of these Lipschitz exponents, we expect a single peak corresponding with the smoothness of the sharpest edges. When we have synthetic test images with large constant regions and step edges, we only have one kind of transitions, namely those step edges. When these edges are blurred, we obtain a histogram with one peak, corresponding with the sharpness of the blurred edges. This is illustrated in fig. (3). In reality, we have a certain distribution around this peak, from which we want to estimate the blur.

Both the position of the maximum in the histogram and the center of gravity (CG) of the histogram are related to the blur in the image, but from experiments, the CG was the most reliable parameter. Let N_k be the number of transitions along significant edges in the image with Lipschitz exponent α_k, then CG is:

$$CG = \frac{\sum_k N_k \alpha_k}{\sum_k N_k} \quad \ldots(9)$$

5 System Implementation:

We studied a test set of eight images, taken from the Kodak website [11] and were taken with digital cameras. From these images, square regions were selected to reduce computation time. In each experiment, an image from this set was blurred with a gaussian PSF with σ_{bl} varying between 1 and 5. Each time, the Lipschitz exponents were calculated among the edges in the blurred image.

For control purposes, they were plotted in a Lipschitz representation image, where intensity is associated with the magnitude of the Lipschitz exponent. We made the histogram and calculated the CG the histogram.

An example of such an experiment for blurring with a Gaussian PSF with variance σ_{bl} _ 3 is shown in fig. (4). In fig. 4(a) the original image is shown, in fig. 4(b) we see the blurred image with σ_{bl}=3. In fig. 4(c), a representation is made of which exponents contribute to the histogram in fig. 4(d). In this representation, the Lipschitz exponent is plotted with black points corresponding to the sharpest transitions in the image; the smoother the transition, the lighter color was used. When fig. 4(c) is compared to fig. 4(a), one can verify that the considered Lipschitz exponents are indeed located among the sharpest edges with large amplitude in the image, though not all edges are found in 4(c) and not all dark points in 4(c) are edges. In our method, this is not a problem, since they are only used for gathering statistics.

We calculated the Lipschitz exponent that corresponds to CG of the histogram, and determined the average $CG\sigma_{bl}$ over the whole set of test images blurred with the same σ_{bl} . To these data $(\sigma_{bl}, CG\sigma_{bl})$, an exponential curve was fitted (fig. 5) experimentally, where the standard deviation over the experiments is shown as a vertical error bar. The fitting was:

$$\sigma_{bl} = a \exp(b\, CG_{\sigma_{bl}}) \quad \ldots(10)$$

in addition, for the parameters the fitting produced a=0.6645 and b=2.6142.

If we compare the estimated σ to the input σ with which the images were originally blurred, we obtain the graph in

fig. (6). In this graph, we can see that the estimations for σ_{bl} are accurate to about 10%. When we plot for all the images in all blurring experiments the estimated sigma versus the input sigma, we see that all the curves are parallel. This suggests that in some images, there was already some initial blur (see top set of curves in fig. (7)). When this offset is subtracted from all curves, the standard deviation is a lot smaller (lower set of curves in fig. (7)). So what we estimate is the total effect of the blur that was already present in the original digital image, and the synthetic blur from the experiment.

When we applied this method to estimate the blur in blurred images for which no blur information was available, it was possible to use this estimation in a classical restoration scheme, and good restoration results were obtained. In fig. (7), a confocal microscope image of a cell nucleus of *Arabidopsis Thaliana* is shown.

The left image shows the raw microscope image, the right image shows the image, restored with the well known Richardson-Lucy restoration algorithm [12], using the raw image and our estimate of the PSF as inputs. As reference image, we manually restored the image with a synthetically generated Gaussian PSF, with σ_{bl} varying between 1 and 15. The image that was restored best, was the one with the same σ_{bl} as the one estimated with our method.

We also tried to estimate the PSF in case of out-of-focus blur. This kind of blur is encountered in auto focus applications, and is modeled by a uniform circular PSF [5, 6].

$$\mathrm{PSF}(x,y) = \begin{cases} K & \text{if } \sqrt{x^2+y^2} < d/2 \\ 0 & \text{elsewhere} \end{cases} \quad \ldots(11)$$

with d the diameter of the focal spot, and K a factor, chosen such that the norm of the PSF is 1.0. In most autofocus applications, one does not estimate the PSF of the blurring, but one only tries to determine if an image is in focus or not. Nevertheless, it is possible to retrieve more information about the blurring, and to use it to adjust the focus more accurately. We repeated the same experiment as before, but this time with synthetic out-of-focus blur. In this case, relation 6 is not valid anymore. For out-of-focus blur, a polynomial provided a good fit to the data:

$$r_{focal} = 19.7\,CG^3 - 19.1\,CG^2 + 17.3\,CG - 2.3 \quad \ldots(12)$$

Using this relation, we can estimate r_{focal}. In fig. (8) a comparison is given between the input blur and the estimated blur. The error bars show the standard deviation over the test set of images used before.

6 Conclusions:

In the experiments, we see that the CG of the histogram of Lipschitz exponents calculated among the edges in the image is a reliable parameter to estimate σ of gaussian blur.

However, the standard deviation on the estimate increases as σ increases. The tests were performed only for vertical edges in the image. Applying the algorithm to horizontal edges is similar, and will allow us to study Gaussian PSF's that are not circular symmetrical (with $\sigma_x \neq \sigma_y$).

References

1. Xiong Y. and Shafer S., 1993, "*Depth from focusing and*

defocusing," in *Proc. of IEEE Conf. on Computer Vision and Pattern Recognition.*

2. Schechner Y. and Kiryati N., 1998, "*Depth from defocus vs. stereo: How different really are they?*" in Proc. International Conf. on Pattern Recognition.
3. Elder J. and Zucker S., 1998, "*Local scale control for edge detection and blur estimation*", IEEE Trans. Pattern Analysis and Machine Intelligence, vol. 20, no. 7, pp. 699–716.
4. Kayargadde V. and Martens J. B., 1994, "*Estimation of edge parameters and image blur from local derivatives*" Journal on Communications, pp. 33–34.
5. Savakis A. and Trussell H. J., 1993, "*Blur identification by residual spectral matching*", IEEE Tans. ImageProcessing, vol. 2, no. 2, pp. 141–151.
6. Savakis A. and Trussell H. J., 1993, "*On the accuracy of psf representation in image restoration*" *IEEE* Tans. Image Processing, vol. 2, no. 2, pp. 141–151.
7. Strela V., Heller P.N., Strang G., Topiwala P., and Heil C, 1995, "*The application of multiwavelet filter banks to image processing*", Technical report, Massachusets Institute of Technology, USA, Submitted to IEEE transform on Image Processing.
8. Mallat S. and Zhong S., "*Characterization of signals from multiscale edges*" IEEE Trans. Pattern Analysis and Machine Intelligence, vol. 14, no. 7, pp. 710–732.
9. Mallat S. and Hwang W. L., "*Singularity detection and processing with wavelets*" IEEE Trans. Information Theory, vol. 38, no. 8, pp. 617–643.
10. Mallat S., *1999, "A wavelet tour of signal processing"*, (2nd ed.), Academic Press, Oval Road, London.
11. "*Kodak digital camera sample pictures*" http://www.kodak.com/digitalIma ging/samples/ lassic.shtml.
12. Van H.T.M. Voort D. and Strasters V., 1997, "*A quantitative comparison of image restoration methods for confocal microscopy*" Journal of Microscopy, vol. 185, no. 3, pp. 354–365.

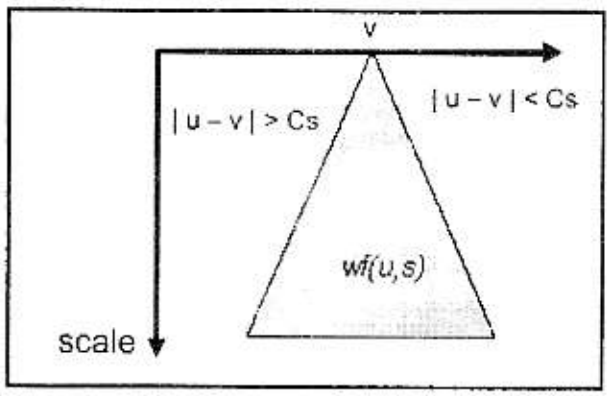

Figure 1. Cone of influence for a point v.

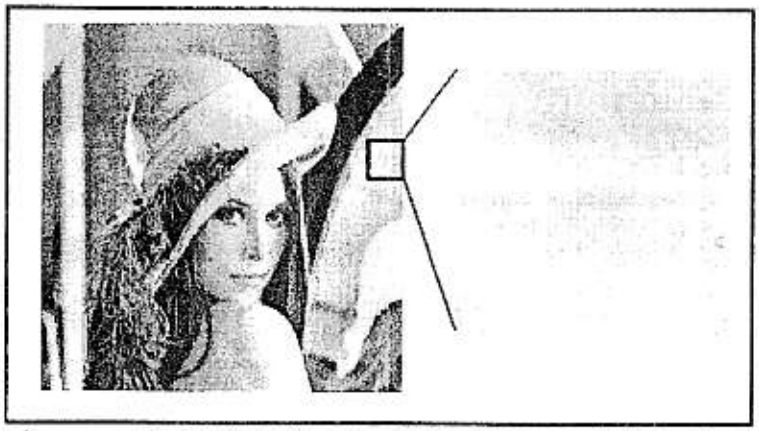

Figure 2. Lena image and detail (mirror) which shows small intensity variations that disturb the blur estimation.

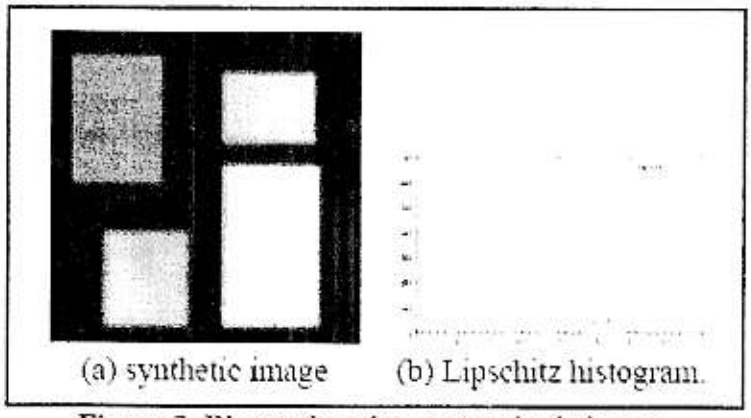

Figure 3. Blur estimation on synthetic image.

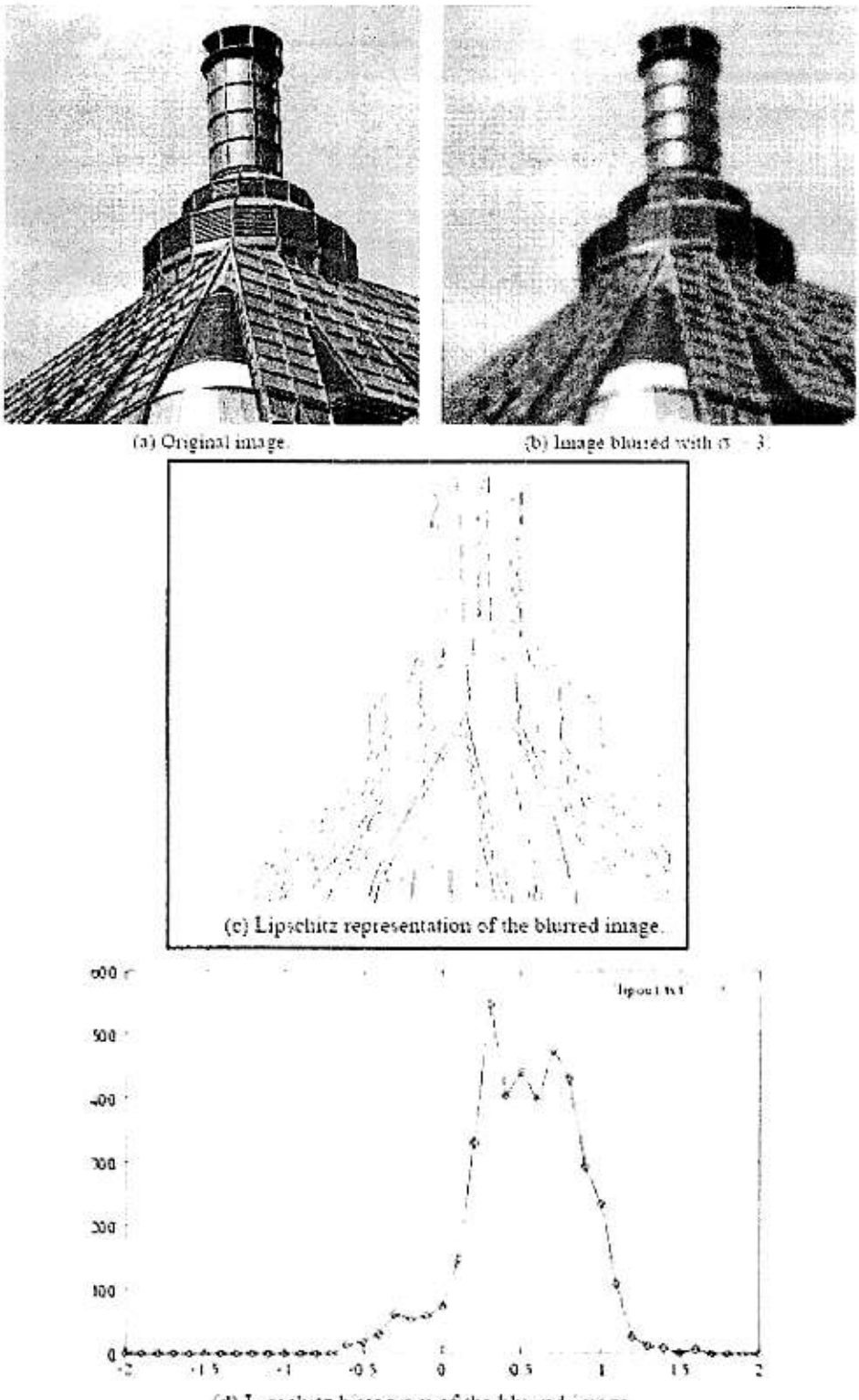

(a) Original image. (b) Image blurred with σ = 3.

(c) Lipschitz representation of the blurred image.

(d) Lipschitz histogram of the blurred image.

Figure 4. Example of a blur estimation experiment on a test image.

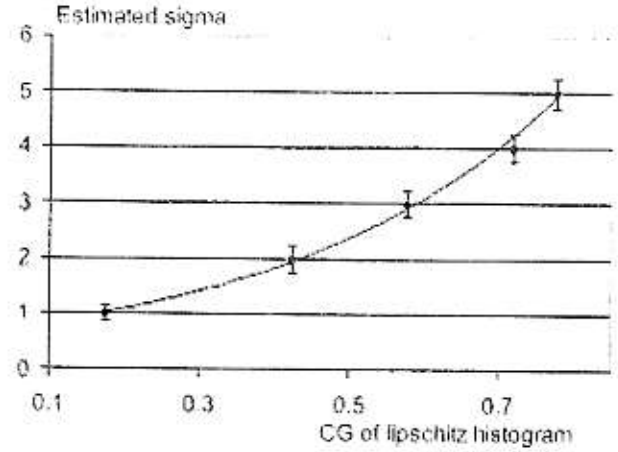

Figure 5. The graph that shows the fitted relation between the estimated σ and CG of the histogram of Lipschitz exponents.

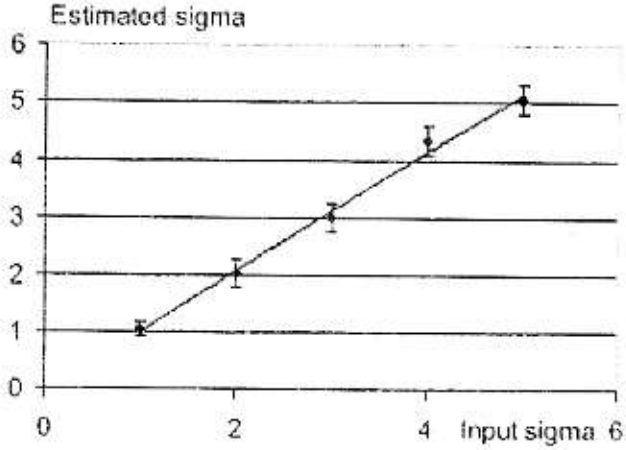

Figure 6. Verification: the estimated σ_{bl} in function of the input σ_{bl} are on a perfect line .

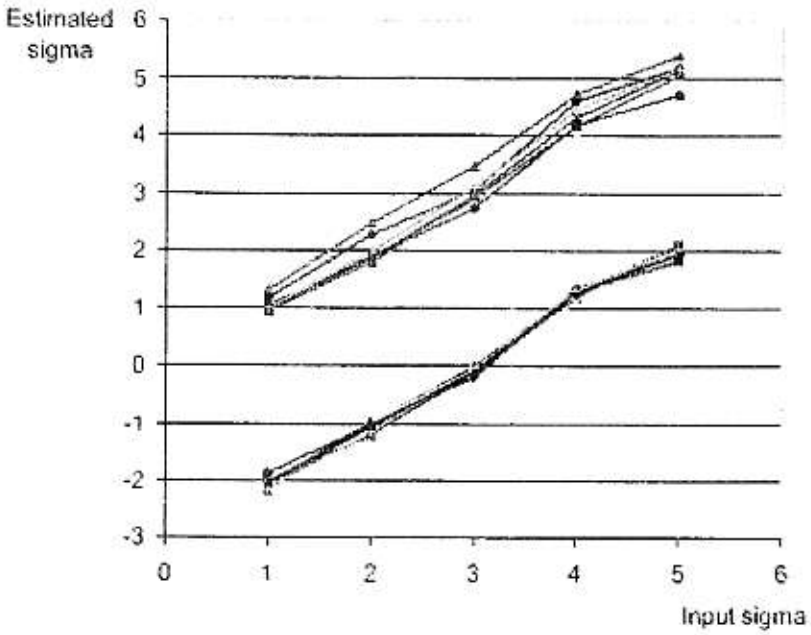

Figure 7. Illustration of the offset effect when comparing the different images. The top set of curves is without subtracting the offset; the bottom set is after subtraction.

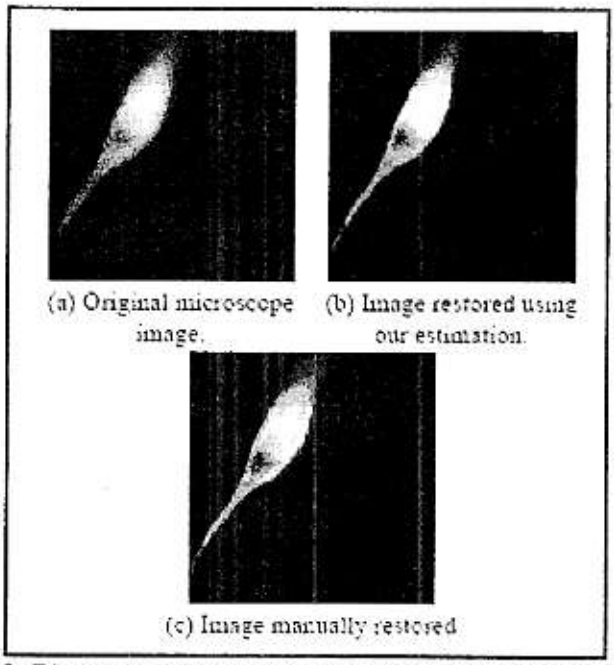

Figure 8. Blur estimation used in restoration of a real image.

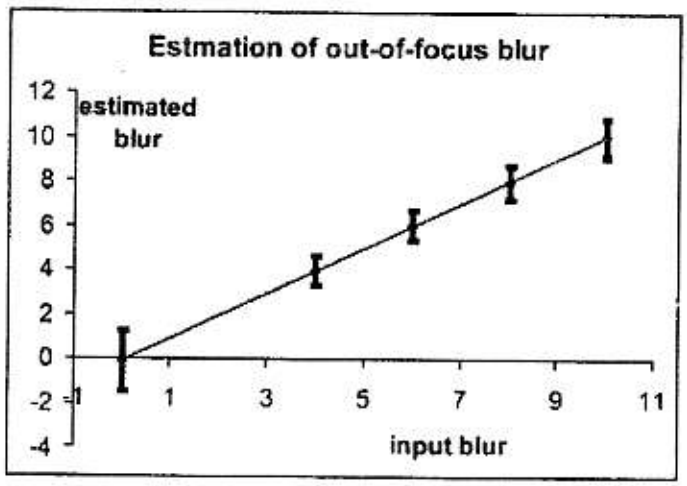

Figure 9. Focus estimation vs real size of the focal spot.